© 2017. Published by The Company of Biologists Ltd | Journal of Experimental Biology (2017) 220, 3327-3335 doi:10.1242/jeb.163824

RESEARCH ARTICLE

Molecular and ultrastructural studies of a fibrillar collagen from octocoral (Cnidaria)

Joseph P. R. O. Orgel[1,2,3,*], Ido Sella[4], Rama S. Madhurapantula[2], Olga Antipova[2,3], Yael Mandelberg[4], Yoel Kashman[5], Dafna Benayahu[6] and Yehuda Benayahu[4,*]

ABSTRACT

We report here the biochemical, molecular and ultrastructural features of a unique organization of fibrillar collagen extracted from the octocoral *Sarcophyton ehrenbergi*. Collagen, the most abundant protein in the animal kingdom, is often defined as a structural component of extracellular matrices in metazoans. In the present study, collagen fibers were extracted from the mesenteries of *S. ehrenbergi* polyps. These fibers are organized as filaments and further compacted as coiled fibers. The fibers are uniquely long, reaching an unprecedented length of tens of centimeters. The diameter of these fibers is 9±0.37 μm. The amino acid content of these fibers was identified using chromatography and revealed close similarity in content to mammalian type I and II collagens. The ultrastructural organization of the fibers was characterized by means of high-resolution microscopy and X-ray diffraction. The fibers are composed of fibrils and fibril bundles in the range of 15 to 35 nm. These data indicate a fibrillar collagen possessing structural aspects of both types I and II collagen, a highly interesting and newly described form of fibrillar collagen organization.

KEY WORDS: Fibrillar collagen, X-ray diffraction, Microscopy, Soft coral, D-period, Red Sea

INTRODUCTION

Collagens are a heterogeneous family of extracellular matrix proteins and are abundant in a plethora of species, ranging from bacteria and fungi to invertebrates and vertebrates. (Exposito et al., 2010). The collagen family is divided into fibrillar and non-fibrillar categories based on packing and ultrastructure. Fibrillar type I collagen is the single most abundant protein (by mass) in animals. A characteristic feature of the fibrillar collagen molecule is its triple-helical domain, where three collagen polypeptide chains are wound around one another to form a rope-like super-helix. The polypeptide chains predominantly contain a repeating glycine (G)-X-Y peptide sequence, where the X and Y positions are usually occupied by proline (P) and hydroxyproline (O). This organization is important for the proper formation of the collagen helix. The GPO sequence is prominent in the C-terminal region, where several successive GPO repeats appear to drive triple-helix polymerization (Swatschek et al., 2002).

Fibrillar collagens are hierarchically organized with a higher order in axial packing to form long fibers. Type I collagen molecules are packed into a quasi-hexagonal array featuring microfibrils of 4–5 nm in diameter (Orgel et al., 2006). The fibrils are composed of microfibrils made of five D-staggered neighboring collagen molecules, where D is normally ∼67 nm, forming the Hodge–Petruska scheme of axial organization. This consists of five molecular segments within an overlap region and four in the gap, which is easily recognized by transmission electron microscopy (TEM) (Petruska and Hodge, 1964).

The occurrence of fibrillar (such as type I) and the basement membrane (type IV) collagens has been described in the earliest branching multicellular animals, namely, Porifera and Cnidaria (Exposito et al., 2008). The body wall of cnidarians is organized from an epithelial bilayer with an intervening acellular component, featuring mainly mesoglea that contain tiny, dispersed collagen fibers (Fautin and Mariscal, 1991). These fibers are markedly different in appearance from cord-like collagen fibers (CLCF). Collagen fibers may appear histologically similar in the mesoglea of different cnidarian species, but can exhibit biochemical features of either fibrillar or basement membrane matrices, creating a structure of scattered and/or organized short fibers that are microscopic in size (Fabricius and Alderslade, 2001).

Current insights into the fibrillar packing of collagen found in the mesoglea of cnidarians come mainly from studies on *Hydra* and jellyfish. However, analogous data are very limited for collagen from *Sarcophyton* species. A search on the taxonomy browser on NCBI (http://www.ncbi.nlm.nih.gov/) revealed that even with widely expanding genomic knowledge, only a few genes/proteins were identified for *Sarcophyton* species (Octocorallia, Alcyonacea), none of which are related to the collagen family. Mandelberg et al. (2016) described microanatomical and biochemical properties of collagen fibers extracted from *S. auritum* colonies. Other works on collagen isolated from the *Sacrophyton* species have been used in making composites for soft-tissue biomimetics (Sharabi et al., 2015, 2016).

The hallmark function of collagen fibers embedded in the mesoglea of these cnidarians is to provide structural support. Long fibers are easily visible when a shallow perpendicular surface rupture of the coral colony is conducted. The fibrillar packing of collagen fibers in the mesentery of *S. ehrenbergi* is largely similar to that found in *S. auritum*, at a microscopic level. The anatomical localization of these fibers is also similar between these species (Mandelberg et al., 2016). However, the molecular and ultrastructural organization of these CLCF differ markedly from the tiny collagen fibers embedded within the cnidarian mesoglea, notwithstanding their biochemical similarities (Exposito et al., 2010).

[1]Departments of Biology, Physics and Biomedical Engineering, Illinois Institute of Technology, Chicago, IL, USA. [2]Pritzker Institute of Biomedical Science and Engineering, Illinois Institute of Technology, 3440 S. Dearborn Ave, Chicago, IL 60616, USA. [3]BioCAT, Advanced Photon Source, Argonne National Laboratory, IL, USA. [4]School of Zoology, George S. Wise Faculty of Life Sciences, Tel Aviv University, Ramat Aviv, Tel Aviv 69978, Israel. [5]School of Chemistry, Faculty of Exact Sciences, Tel Aviv University, Ramat Aviv, Tel Aviv 69978, Israel. [6]Department of Cell and Developmental Biology, Sackler School of Medicine, Tel Aviv University, Tel Aviv 69978, Israel.

*Authors for correspondence (orgel@iit.edu; YehudaB@tauex.tau.ac.il)

J.P.R.O.O., 0000-0002-1050-9391

Received 29 May 2017; Accepted 6 July 2017

Journal of Experimental Biology (2017) 220, 3327-3335 doi:10.1242/jeb.163824

In the present study, we elaborate on the unique molecular and ultrastructural organization of CLCF isolated from the reef-dwelling octocoral *S. ehrenbergi* (v. Marenzeller 1886). This species grows in well-illuminated parts of the reef into mushroom-shaped colonies (Fig. 1A). The gastrovascular cavity of these cnidarians consists of cord-like fibers stretching out from the mesenteries, which are visible to the naked eye (Fig. 1B). These fibers can be observed upon performing a shallow incision of the polyp surface, perpendicular to the long axis. The pulled fibers may reach a few tens of centimeters in length, and thus differ from the common thinner and much shorter fibers found in the mesoglea. The ultrastructural analyses presented here are supported by the similarity in amino acid content of these fibers to other fibrillar collagens, as determined by high-performance liquid chromatography (HPLC). This further validates the use of molecular structure and packing information previously collected for type I and II collagen (structure factors and phases) to determine the packing features of this plausibly novel class of collagen from *S. ehrenbergi*.

The fibers isolated from *S. ehrenbergi* were stained with Masson's Trichrome, a classic histological stain for fibrillar collagen. TEM was also performed on these fibers, which demonstrated the typical pattern of D-periodic striation and parallel fibers arrangement as known for mammalian fibrillar collagen type I. Biochemical analyses show that these fibers indeed belong to the fibrillar collagen subfamily.

Molecular packing features of these fibers were obtained with the use of X-ray fiber diffraction (XRD). These data suggest that aspects of vertebrate type I and II collagen packing can be observed in these CLCF. The unique XRD patterns and the one-dimensional electron density profiles constructed from them suggest that these cord-like fibers are formed from a fibrillar collagen similar to that seen in vertebrates. We present here the first data to demonstrate molecular packing of these long CLCF obtained from *S. ehrenbergi*, which has features of fibrillar packing observed in type I and II collagen, while not being clearly one type or the other as judged from the structural data presented here (Sella, 2012).

MATERIALS AND METHODS

Methods for sample collection, histology, microscopy and amino acid analysis were reported in Mandelberg et al. (2016) for the analysis of fibers obtained from *S. auritum*. These methods can be applied for similar analysis on fibers extracted from *S. ehrenbergi*, as these organisms belong to the same genus.

Sample collection

Fragments of *S. ehrenbergi* (3–4 cm^3) were removed from the polyp-bearing part of the colony as previously described (Fabricius and Alderslade, 2001). Samples were collected from the reefs of Dahalak Archipelago (southern Red Sea) and Eilat (Gulf of Aqaba, northern Red Sea) at a depth of 3–5 m. They were individually placed, underwater, into zip-lock bags and immediately brought to the Benayahu laboratory at Tel Aviv University for further processing. Collection of animals complied with a permit issued by the Israel Nature and National Parks Protection Authority.

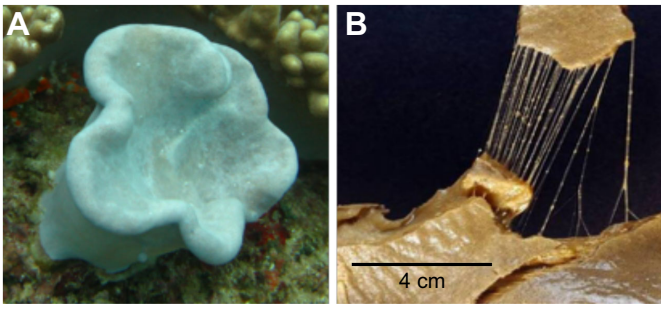

Fig. 1. Collagen fibers from *Sarcophyton ehrenbergi* colonies. (A) Underwater image of the octocoral *Sarcophyton ehrenbergi*. (B) Torn-apart colony revealing collagen fibers.

Histological evaluation of the gastrovascular cavity

Samples were removed from colonies that had been previously preserved in 4% glutaraldehyde in seawater. These samples were decalcified, twice, by incubating them in a mixture of equal volumes of formic acid (50%) and sodium citrate (15%) for 20 min, and then transferred back to 4% glutaraldehyde. They were then rinsed with distilled water, and embedded in 2% agarose (50°C) or in high melting point paraffin. Following solidification, rectangular pieces, closely fitting around each sample, were cut out and dehydrated using a graded series of ethanol. The samples were then embedded in paraffin. Cross-sections of 5–8 µm were prepared using an M1R microtome (Shandon, Thermo Fisher Scientific, Waltham, MA, USA). Sections were stained with Manson's Trichrome, which stains collagen (Ross and Pawlina, 2006).

Light microscopy on isolated fibers

Isolated fibers were fixed in 4% formaldehyde in seawater, rinsed with distilled water, and preserved in 70% ethanol. The subsamples were placed in paraffin (56°C) and 6–7 µm cross-sections were obtained using a microtome (M1R, Shandon). The sections were stained with Masson's Trichrome (Ross and Pawlina, 2006). Fibrillar collagen is stained with a turquoise color with this histology stain. These stained sections were examined under an Optiphot microscope (Nikon, Japan) (Mandelberg et al., 2016).

Protein and amino acid analysis

In order to characterize the protein that composes the fibers, amino acid analysis was performed at the Department of Chemical Research Support, Weizmann Institute of Science (Rehovot, Israel). The method described in Bütikofer et al. (1991) was employed to determine amino acid composition and free amino acids in protein hydrolysates (Bütikofer et al., 1991).

Briefly, hydrolysates were prepared by treating the crushed fibers with several volumes of tri-sodium citrate di-hydrate for a short time and then diluting this mixture using deionized water. Internal standards were then added to the mixture, which was then incubated at 40°C with occasional mixing. Sensitive detection and separation of hydrolyzed samples (amino acids) were achieved with the use of HPLC. The chromatographic column was preptreated with ophthalaldehyde, 3-mercaptopropionic acid (OPA/MPA), and 9-fluorenyl-methyl chloroformate (FMOC). The pre-column preparation was fully automated and had a detection range of 100–3000 pmol, thus requiring only a small sample (1 µl). Three samples of isolated collagen fibers (ca. 5 µg each) from samples collected at different collection sites were analyzed using a Waters PicoTag Work Station for gas phase hydrolysis and a Hewlett Packard 1090 HPLC equipped with a diode array detector and an auto injector with a PC-based Chemstation database, utilizing Amino Quant chemistry.

Ultrastructure analyses

Scanning electron microscopy

For scanning electron microscopy (SEM), samples from the polypary, ~3 cm^2 each, and isolated fibers were fixed in 4%

Journal of Experimental Biology (2017) 220, 3327-3335 doi:10.1242/jeb.163824

glutaraldehyde in filtered seawater (0.22 µm FSW). These samples were dehydrated through a graded series of ethanol (up to 100%), and critical-point dried with liquid CO_2. The polypary preparations were fractured using the tips of fine forceps to expose the gastrovascular cavities. These samples were coated with gold for SEM evaluation (JSM-840A, JEOL USA, Peabody, MA, USA). In addition, fibers were dehydrated as described above, coated with a gold-palladium alloy for environmental SEM (E-SEM) evaluation (JSM-6700 Field Emission SEM, JEOL USA). Measurements on fiber and fibril diameters were performed using the ImageJ program (Schneider et al., 2012).

Transmission electron microscopy

Samples were fixed as described above and then decalcified, twice, in a mixture of equal volumes of 50% (v/v) formic acid and 15% (w/v) sodium citrate for 20 min, and then placed in 4% glutaraldehyde and dehydrated through a graded series of ethanol (Dykstra and Reuss, 2003). The samples were embedded in EPON liquid epoxy resin and the sections were stained with both uranyl acetate and lead citrate. Glycoproteins were detected using Sodium Tungstate and Cupromeronic Blue staining (Scott, 1990). Negative staining was employed to study fibrils that were detached from fibers by sonication at 30 kHz for 5 min (PCI 1.5, PCI Analytics, Mumbai, India) (Ortolani and Marchini, 1995). TEM was carried out on a JEOL 1200 EX electron microscope.

X-ray fiber diffraction data

XRD on dry collagen fibers from *S. ehrenbergi* was performed at the Biophysics Collaborative Access Team (BioCAT, ID18) and the Biology Center for Advanced Radiation Sources (BioCARS, ID14) at the Advanced Photon Source, Argonne National Laboratory, Chicago, IL, USA (Barrea et al., 2014). Similar diffraction data from native, hydrated rat tail tendon and lamprey notochord were obtained from previous studies (Orgel et al., 2000, 2006; Antipova and Orgel, 2010) and from linked RCSB codes (3HR2 and/or 3HQV). The scaled amplitudes of the central, meridional section of each data set were used to calculate electron density maps. These data for type II collagen were published as supplementary information to Antipova and Orgel (2010). Electron density maps were calculated according to the methods published previously (Antipova and Orgel, 2010).

Comparison between X-ray- and TEM-derived electron densities

A one-dimensional line profile was computed from TEM images of thin-fibrils across ~220 nm for an exceptionally well resolved fibril. The region corresponding to two D-periods (each D-period of ~67 nm) was recognizable. The average line profiles for these D-periods were then compared with the analogous D-period line profile, i.e. a one-dimensional electron density map, obtained from the combination of structure factors as explained in the Results.

RESULTS

Histological evaluation of collagen fibers

To establish the localization and type of collagen (fibrillar or network forming) in the mesentery of *S. ehrenbergi*, Masson's Trichome staining was performed. A histological cross-section of the uppermost part of a polyp below the pharyngeal level reveals the free edge of the mesenteries, which are directed towards the center of the gastrovascular cavity (Fig. 2A). The mesenterial filaments of six out of the eight mesenteries feature an inner part, which when stained by Masson's Trichrome, give a specific turquoise color. This is indicative of the presence of collagen. The fibers pulled out

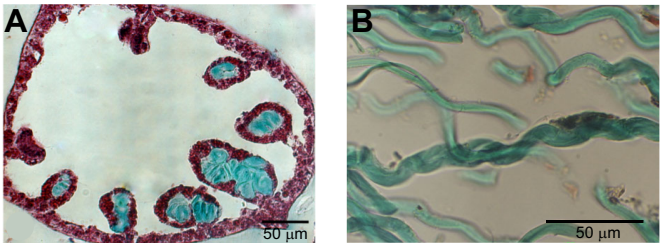

Fig. 2. Collagen staining in *S. ehrenbergi* mesenteries and isolated fibers. (A) Masson's Trichrome-stained histological cross-section of uppermost part of a polyp below the pharyngeal level reveals free edge of mesenteries loaded with turquoise-stained collagen fibers directed towards the center of the gastrovascular cavity; light-stained periphery indicates the non-fibrous collagen. (B) Isolated fibers stained with Masson's Trichrome resulted in turquoise color, indicative of collagen.

from the polypary of *S. ehrenbergi* exhibit bundles, each comprising numerous fibers (Mandelberg et al., 2016; Sharabi et al., 2014). Isolated fibers (Fig. 1) stained with Masson's Trichrome resulted in the same turquoise color, indicative of collagen (Fig. 2B). The fibers are approximately 9 µm in diameter and they form bundles with a width of 100–200 µm, resembling coiled structures, as seen in TEM micrographs (see Ultrastructural analysis using electron microscopy, below) (Mandelberg et al., 2016; Sella, 2012). This arrangement of fibers is used as a hydroskeleton to support the colonies biomechanically. In addition, these fibers also accommodate the extra load rendered by the gonads borne by the mesenteries. The coiled collagen fibers within the mesenteries have already been described for *S. auritum* (Mandelberg et al., 2016), but have not been described in any other cnidarian or invertebrate. Therefore, it seems that the new structure and arrangement of the fibers reported here are unique both in their location and structure in the soft coral colony and thus are important for the soft coral structure.

Protein and amino acid analysis

Twenty-seven distinct peaks were recorded on the HPLC profile (Fig. 3). Nineteen of these peaks were recognized and quantified. The unidentified peaks might be a result of additional amino acids, which are common in marine organisms and are known as

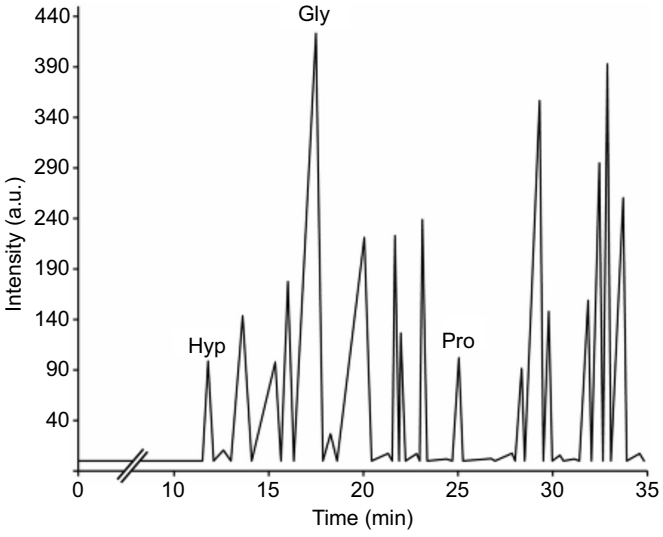

Fig. 3. HPLC profile from hydrolysate of fibers. This profile was analyzed using the Chemstation Database and the glycine (Gly), proline (Pro) and hydroxyproline (Hyp) are marked.

Journal of Experimental Biology (2017) 220, 3327-3335 doi:10.1242/jeb.163824

Table 1. Comparison of amino acid content between *Sarcophyton ehrenbergi* collagen, type I collagen from rat tail tendon (RTT) and human type II collagen

	Amino acid content (%)		
	S. ehrenbergi	RTT Type I collagen	Human type II collagen
Hpro	4.15	9.96	NA
Asp	8.34	1.53	1.67
Ser	4.35	4.18	3.27
Glu	9.52	4.56	5.18
Gly	24.89	33.22	31.87
His	0.94	0.41	0.56
Arg	5.35	4.95	5.02
Thr	3.43	2.04	2.31
Ala	6.49	10.53	9.96
Pro	5.08	12.00	21.27
Tyr	1.52	0.35	0.64
Val	3.97	2.36	1.43
Met	1.96	0.67	0.56
Lys	2.96	2.97	3.67
Ile	2.47	1.12	1.59
Leu	3.29	2.39	2.63
Phe	1.69	1.21	1.04

non-proteinogenic amino acids (NPAA) (Nelson et al., 2003). NPAA are typically formed as a result of post-translational modifications or as intermediates in metabolic processes (Curis et al., 2005). Hydroxyproline is one such NPAA that is important for stabilizing the packing structure of fibrillar collagens, as it participates in the formation of enzymatic crosslinks (Orgel et al., 2000). Aeration of peptide bonds by seawater also results in the modification of amino acids in these organisms (McDowell et al., 1999).

High concentrations of glycine, proline and hydroxyproline, relative to non-collagenous proteins, are similar to concentrations of these amino acids in other fibrillar collagens (Table 1). The overall similarity in the amino acid content from *S. ehrenbergi* in comparison to rat type I and human type II collagen suggests that the molecular and fibrillar packing structure of collagen in these fibers is indeed similar. A comparison between the amino acid content of the *S. ehrenbergi* collagen presented here and other fibrillar and network-forming collagens is discussed in Appendix 1 (see Table A1).

Ultrastructural analysis using electron microscopy

The micrographs of fibrils in longitudinal sections exhibited a repeating pattern of dark and light banding perpendicular to the fiber axis and are reminiscent of the fibrillar collagen D-band repeat that were not homogeneously stained as is typical in collagen. The diameter of the fibrils in the cross-sections was 15.16±3.41 nm (n=17 fibrils in six fibers; Fig. 4D) and the width of thin fibers in the longitudinal sections was 15.9±3.11 nm (n=15 fibrils in three fibers; Fig. 4E).

An E-SEM analysis revealed that the fibrils are interwoven to form a three-dimensional arrangement, with free ends on some fibrils, and fused or bifurcated ends on others (Fig. 4F). Such an arrangement adds to the mechanical properties of the fibers and caters to the wide range of tensile stresses that octocorals experience in their natural environment. The presence of ends and bifurcations was evident in the fibers, displaying morphological features that are typical for growing fibers, as described in Mandelberg et al. (2016). Similar bifurcations and (fibril) fusions occur during the formation of new collagen fibers in developing fetuses, in growth, and in the regenerating scar tissues of mammals [e.g. rat (Provenzano and Vanderby, 2006) and sheep (White et al., 2002)]. This would appear to be a feature shared between these octocoral collagen fibrils and fibers and the equivalent collagen fibrils and fibers of vertebrates. The average fibril and fibril-bundle (fiber) diameter measured from E-SEM images ranged from 14.48 to 38.93 nm, which correlates with the average diameter measured from TEM images (Fig. 4D).

TEM images of fragments of negatively stained fibrils, isolated by sonication, featured a diameter of 18.9±2.45 nm (n=41 measurements on 27 isolated fibrils; Figs 4 and 5) as well as a repeated dark and light banding perpendicular to the fiber axis. Examination of this banding along the fibrils by creating a color intensity distribution showed dark repeating bands every 65–70 nm (the D-periodic repeat), with some lower amplitude (less dark) repeating bands in the 65–70 nm zone (Figs 4 and 5), suggestive of the pattern of mammalian fibrillar collagen. This D-period value is supported by the X-ray observations (see below). Furthermore, the negative staining of isolated fibrils revealed a parallel arrangement of thinner sub-structures ∼3 nm wide (Fig. 5), protruding from the end of the fibril, which featured an uneven surface area (Fig. 5). This structure resembles that observed for type II collagen (Antipova and Orgel, 2010), where collagen microfibrils are observed at the fractured end of a collagen fibril. Microfibrils have been observed for type I and type II collagen and are believed to be a feature of fibrillar collagen in general, but, for reasons of molecular architecture, are not separable from a type I fibril owing to the cooperative nature of

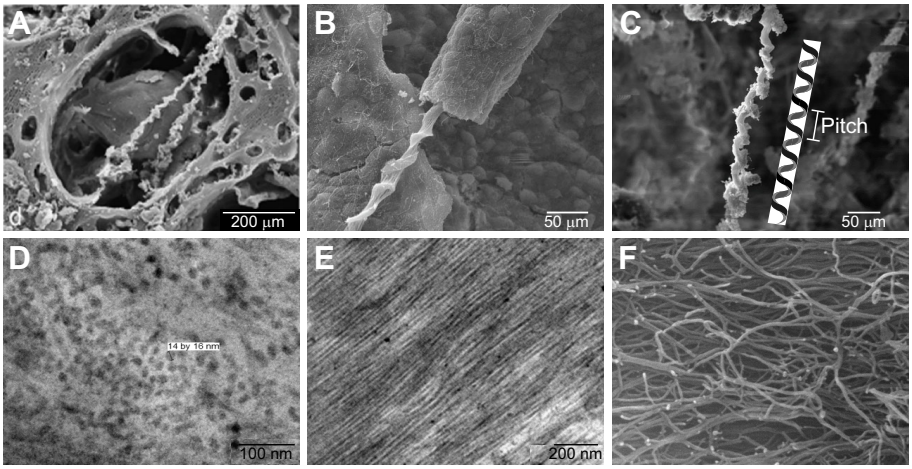

Fig. 4. Electron microscopy of collagen fibers from *S. ehrenbergi*. (A–C) SEM images of fibers emerging from an exposed polyp cavity; the fibrillar texture and the helical structure (pitch as noted in inset in C). (D,E) TEM image of a cross-section (D) and a longitudinal section (E) of a fiber. (F) E-SEM image of isolated collagen fibers showing fibrils exhibiting interweaving configuration with fibril ends and fiber bifurcations.

Journal of Experimental Biology (2017) 220, 3327-3335 doi:10.1242/jeb.163824

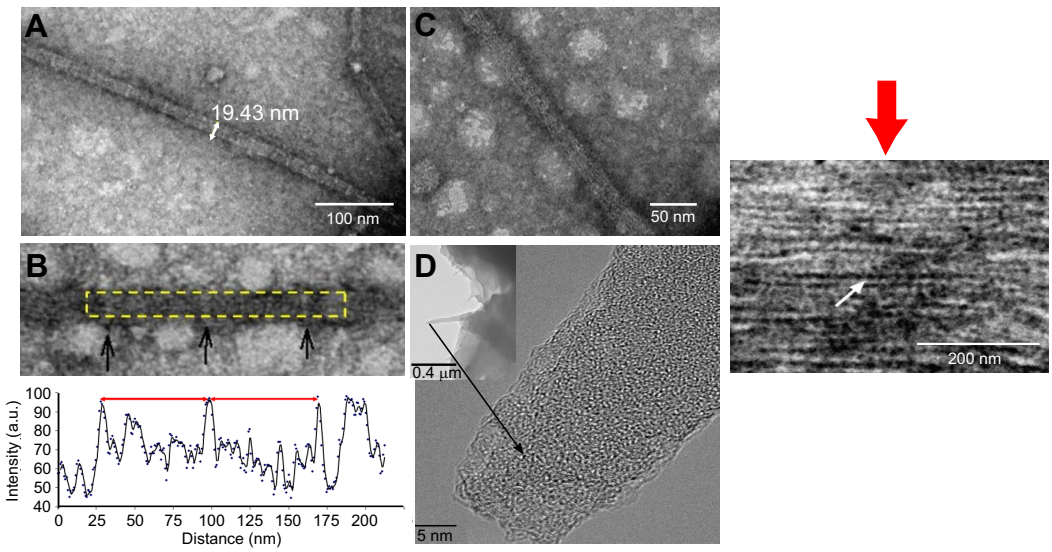

Fig. 5. TEM of *S. ehrenbergi* collagen fibers. (A) TEM micrograph of an isolated positively stained fiber of *S. ehrenbergi*, showing organized D-period substructure. (B) One-dimensional scan of two D-periods (shown below), which assigns relative 'intensity' to the relative electron density of each part of the D-period that is approximately 66 nm in length. (C) Negatively stained fiber, shows composition from still thinner fibers (thin fibrils). (D) 'Ground substance' between collagen fibers, likely composed of GAG-rich proteoglycans. Red arrow: TEM micrograph of an isolated fiber (9 μm diameter) showing organized fibrillar structure and a densly hydrated proteoglycan matrix between fibrils (black, marked by white arrow).

that fibril's construction. In contrast, independent microfibrils have been observed jutting out from the end of a partially disrupted type II fibril.

From the TEM data, it was observed that there was an unstained area between adjacent thin fibers. When stained with Cupromeronic Blue (CB), these fibers exhibit a strong dark blue coloring of proteoglycans (Fig. 4D). Fibers in the longitudinal sections of the CB-stained samples revealed a parallel arrangement of closely packed fibrils surrounded by a dense proteoglycan matrix (as determined from CB staining). This matrix seemed to be distributed evenly between the fibrils and along the fiber (Fig. 5D). When comparing the TEM micrographs of longitudinal sectioned fibers

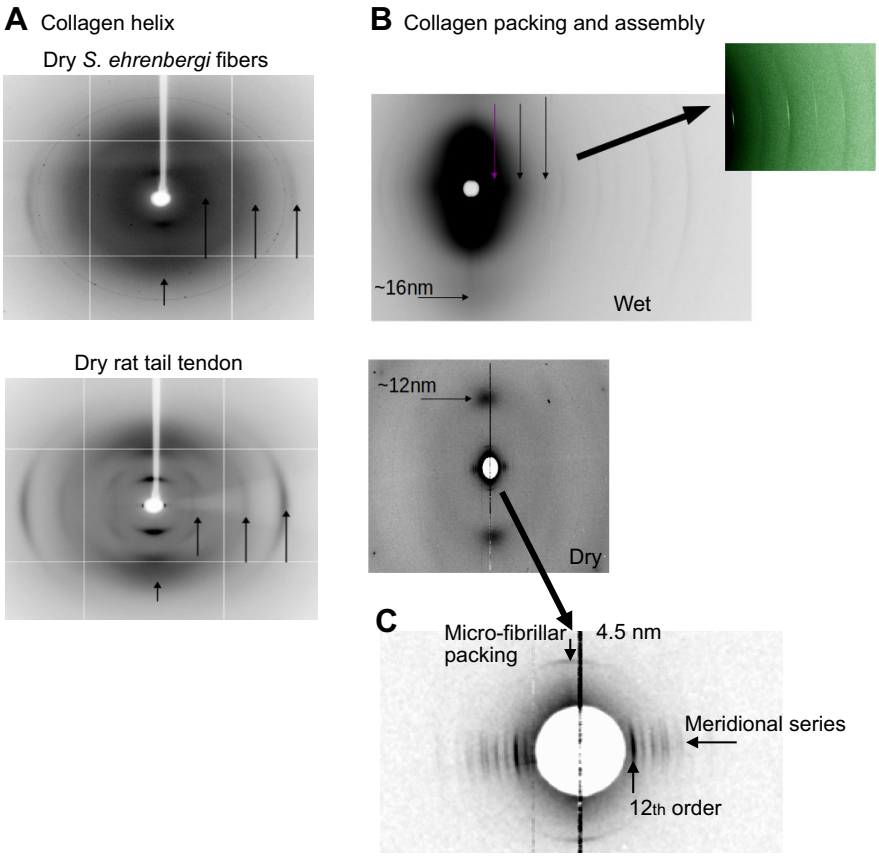

Fig. 6. X-ray diffraction patterns. (A) Wide-angle X-ray diffraction of dry *S. ehrenbergi* fibers and dry rat tail tendon; the helix layer lines/meridional reflections originating from the molecular transform appear to be similar. The three right vertical arrows show (collagen) helix layer lines. The leftmost vertical arrow shows the molecular packing function. (B) Low-angle wet and dry coral fiber diffraction. Note the fibril interference function between 12 and 16 nm. In the fiber diffraction of the wet fibers, the meridional diffraction originating from the D-period is evident, like that seen in rat tail tendon. The first three orders of this diffraction series (vertical arrows; as do meridional orders 3–8 shown in the inset) conform to a periodicity of 66 nm, which is directly analogous to the 67 nm D-periodicity of rat tail tendon. Horizontal arrows show fibrillary packing function; a diffuse fibillar packing function is observed at 16 nm in wet fibers, but 12 nm in dried fibers. Inset: X-ray diffraction low-angle (meridional orders 3–8) comparison of *S. ehrenbergi* (dark) with 66 nm periodicity superimposed on rat tail tendon (light) with its 67 nm periodicity. (C) Medium-angle fiber diffraction of coral fibers. Note the packing function at 4.5 nm, which is the same value seen for the collagen type I and II microfibrils (Antipova and Orgel, 2012; Orgel et al., 2006).

Journal of Experimental Biology (2017) 220, 3327-3335 doi:10.1242/jeb.163824

with CB-stained fibers (Fig. 4), it is evident that CB labeled the areas between adjacent fibrils within the fibers, structured in a manner found commonly in mammalian connective tissue fibrillar collagens.

X-ray diffraction and D-period electron density organization

X-ray diffraction (Fig. 6) revealed a 66 nm meridional periodicity in both wet and dried preparations of octocoral collagen fibers, suggestive of an average molecular tilt of ∼14 deg relative to the fiber axis. This is in contrast to type I–III collagen, which average about a 10 deg molecular tilt from the fiber axis (with a 67 nm D-period) (Wess and Orgel, 2000). The meridional intensity distribution of the octocoral fibers differs from both type I and type II collagen, which suggests that the D-period organization is non-identical (Fig. 6C see 'Meridional series'). The collagen helix layer lines are evident along the fiber axis (Fig. 6A), and the pattern loosely resembles that of rat-tail tendon diffraction, indicating a collagen triple helix (Fig. 6A).

The similiarity in the amino acid content (Table 1) between the *S. ehrenbergi* collagen fibers and mammalian type I (rat) and type II (human) collagen enables the systematic application of crystallographic information collected from the latter to X-ray diffraction and electron microscopy data reported herein. This process, known as molecular replacement, has been used over many decades to arrive at preliminary structures for new proteins (especially extracellular matrix proteins) that share similarities with proteins of known structure (Höhne and Rossmann, 1973; Tickle and Driessen, 1996). Furthermore, there is a stark similarity in the diffraction profile observed between *S. ehrenbergi* fibers and those of type I and II collagens as described in previous works (Antipova and Orgel, 2010, 2012; Orgel et al., 2006). Hence, it is prudent to calculate one-dimensional electron density maps from the data in hand by combining structure factors and phase information from the previous structural determinations of type I and II collagen, with the amplitudes recorded from the octocoral diffraction patterns. This provides a means of estimating and observing the crystalline fibrillar D-periodic packing structure of the octocoral fibers. Fig. 7 shows the one-dimensional electron density profiles calculated using type I and II phases.

The electron density map generated with type I phases is scrambled, i.e. no gap-overlap step function, and is significantly different from the original native type I map. In contrast, there is an intelligible electron density map generated with the phases of vertebrate type II collagen in comparison with that generated from 'random' phases, or with those originating from the structure of type I collagen (Fig. 7). This type II structure based electron density map shows a gap-overlap step function and resembles that of the native type II electron density map. This strongly indicates a fibrillar D-periodic organization of the octocoral fibers and suggests that it may be closer to type II than to type I collagen structure. This alignment of electron density will not happen by pure chance, an estimate of which, conservatively, is of the order of 1 in 6^{13}, assuming 60 deg error per phase, and as is demonstrated by the selected electron density map formed from octocoral amplitudes but randomly generated phases.

An average electron density was calculated from the TEM of coral fibers over two D-periods (Fig. 8). Although it is tempting to point to

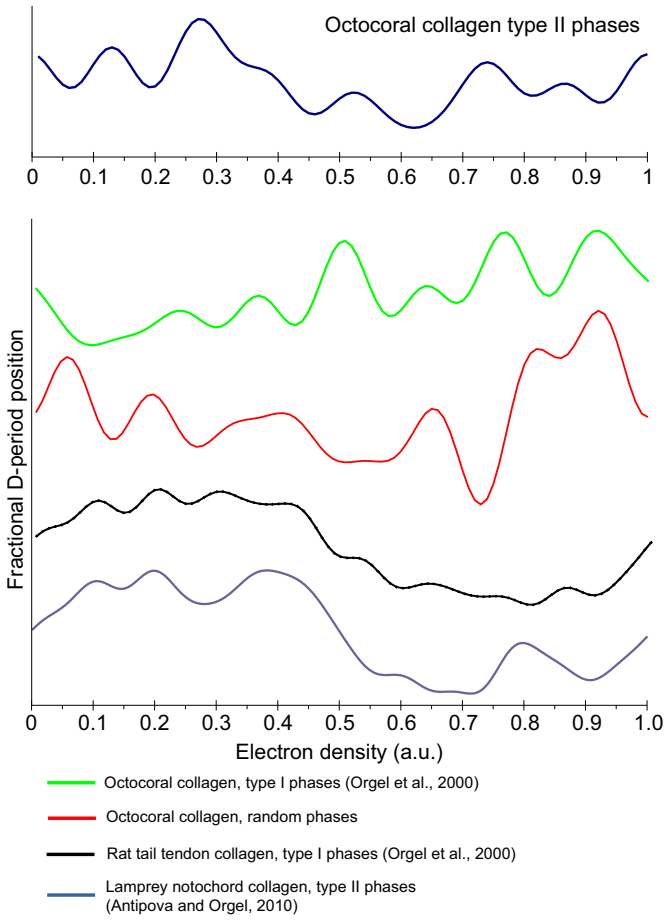

Fig. 7. X-ray derived electron density maps. Extracted amplitudes from the low-angle meridional diffraction pattern of hydrated fibers of *S. ehrenbergi* combined with the phase information from different sources based on the principle of molecular replacement. Here, the phases of type I and type II collagen (rat tail tendon and lamprey notochord) were each combined with the meridional derived amplitudes of the octocoral. A random set of phases was also applied in the same manner for comparison with the Fourier maps generated from the use of the type I and type II collagen phases. The original 1D Fourier maps of type I and type II collagen using their respective amplitude and phase sets as per their original publications are also shown for comparison (see color key). This shows that of the three 'phase replacement' Fourier maps (type I, type II and random phases), the only intelligible one-dimensional Fourier map calculated from the octocoral amplitudes, and the only one that resembles a fibrillar collagen map, is the one with the collagen type II phases (blue). The presence of a gap-overlap in the coral electron density map, while not identical to either the native type I or type II collagen map (black and light blue, bottom) in its D-period organization, does shows enough similarity to imply a common organization in the D-period substructure.

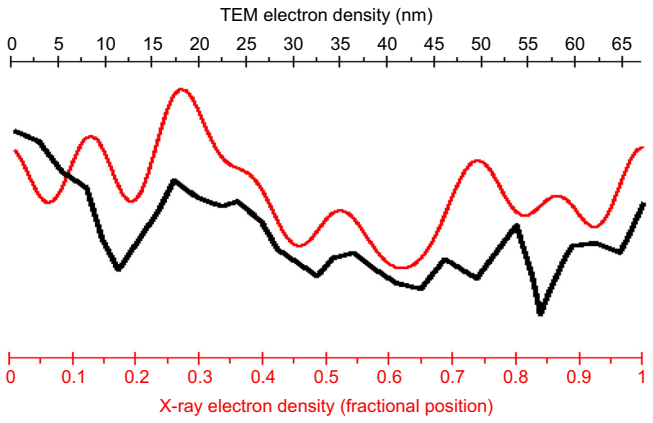

Fig. 8. Comparison of electron densities of the D-period sub-structure of *S. ehrenbergi* fibrils determined from TEM and X-ray diffraction.

Journal of Experimental Biology (2017) 220, 3327-3335 doi:10.1242/jeb.163824

the obvious similarities between the TEM and X-ray derived electron density maps, the fact that the TEM map was derived from only two D-periods (from an exceptionally clear section of TEM data) suggests that there should be great caution in assigning any value to their similarity, other than their gross overall similarity (for instance, the gap/overlap ratio). In this regard, the data obtained from the X-ray diffraction have much greater statistical significance (being derived from the X-ray contribution of millions of crystalline domains within the sample) than those obtained from a TEM observation, even though these TEM observations confirm the X-ray data.

The X-ray diffraction-derived electron density map is still sufficiently different to indicate that there are structural dissimilarities in packing organization, despite its similarity to type II collagen and the apparent organization (and fibril size) that resembles type II collagen, and especially while the helical organization of the octocoral collagen resembles type I collagen (see Fig. 6). These differences may be organizational, compositional or both. They could be due to amino acid content differences in the collagen protein itself and/or the deposition of highly organized ECM ligands such as proteoglycans on the surface of the fibrils/fibril bundles.

DISCUSSION

The cord-like collagen fibers of octocorals exhibit a unique location and arrangement within the mesenteries that are markedly differ from the mesoglea collagen. Their structural organization is unusual among cnidarians and here we demonstrate that they resemble vertebrate collagen in structural organization. It is possible that their intriguing differences in mechanical properties from that of mammalian collagens (Danto and Woo, 1993; Fung and Liu, 1995; Vogel, 2013) could well arise almost entirely from their proteoglycan-rich organization, which might also be the underlying reason for their unique structure. In the mesoglea, fibrils are short and the matrix surrounding them is thick and soft (e.g. *Metridium* mesoglea). As a result, the mesoglea can withstand large strains (deform to several hundred percent extension) by the sliding of fibrils relative to their neighbors. Thus, it appears that the octocoral fibers are an extreme mesoglea component that present tighter structural organization, more similar to that of a vertebrate tendon or ligament.

The difference in properties between the octocoral fibers and the vertebrate fibrillar collagens could be a result of the difference in the structure of collagen fibrils, the matrix between the fibrils, or a combination of both. Nevertheless, it is without doubt (to us) that based on our observations of molecular and structural organization, these coral fibers are much closer to tendon/ligament of vertebrate collagens than to the collagenous mesoglea typically seen in other cnidarians. These are unique fibers, and their role in the coral physiology is enigmatic. The similarity of D-periodic fibril structure between vertebrate type II collagen and this invertebrate form is striking, the major organizational differences perhaps coming from the very rich proteoglycan-mediated organization. However, we cannot rule out the possibility of a unique collagen. Even if this were the case, its fibrillar D-periodic structure is clearly close to that of type II collagen of vertebrates, while the organization into fibril bundles resembles that of type I collagen in tendons and ligaments of vertebrates. Regardless, the vast quantity of these organized bundles of fibers within *S. ehrenbergi* suggests that they do play a significant, yet still unknown role in the octocoral physiology. Given that invertebrates account for at least 95% of all animals, one can readily anticipate that they are a potential treasure trove of unique collagens.

APPENDIX 1

Amino acid sequences of fibrillar and non-fibrillar collagens

Over 25 types of fibrillar and non-fibrillar collagens have been reported in humans. However, only fibrillar (e.g. type I and II) and network-forming (type IV) types of collagen have been reported in the earliest branches of multicellular organisms such as cnidarians (Exposito et al., 2008). The amino acid composition of type IV collagen from humans has been under evaluation for decades. The usual G-X-Y repeat found in fibrillar collagens is often found to be disrupted in human type IV collagen (Glanville, 1987). There are

Table A1. Comparison of amino acid contents between type I (fibrillar) and type IV (network-forming) collagens from *Sarcophyton ehrenbergi* with other species

	S. ehrenbergi	Rat type I collagen (3HR2_A, 3HR2_B)	Human type II collagen (P02458)	Human Col4α1 (AAI51221)	Cnidarian Col4α1* (KXJ15387)
G	24.89	33.22	31.87	28.64	17.80
P	5.08	12.00	21.27	19.47	12.20
Hyp	4.15	9.96	0.00	0.00	0.00
A	6.49	10.53	9.96	3.48	4.27
R	5.35	4.95	5.02	2.70	5.00
E	9.52	4.56	5.18	4.19	3.54
S	4.35	4.18	3.27	4.31	6.71
D	8.34	2.84	3.27	3.48	4.88
K	2.96	2.97	3.67	5.57	7.56
Q	n/a	2.71	2.95	4.31	2.93
T	n/a	2.04	2.31	2.58	4.88
L	3.29	2.39	2.63	5.51	6.22
V	3.97	2.36	1.43	3.06	5.12
F	1.69	1.21	1.04	2.76	1.83
N	n/a	1.53	1.67	0.96	3.29
M	1.96	0.67	0.56	1.86	2.56
I	2.47	1.12	1.59	3.48	4.76
Y	1.52	0.35	0.64	1.08	2.44
H	n/a	0.41	0.56	1.02	1.34
C	n/a	0.00	0.64	1.20	1.46
W	n/a	0.00	0.48	0.36	1.22

The accession numbers of the sequences are indicated in parentheses. Hyp, hydroxyproline.
*Partial sequence available.

considerable differences in macromolecular structure of these two collagen types. These differences are a result of the amino acid composition and positioning of the X and Y amino acids within the G-X-Y repeat itself, between the two types of collagen (Schwarz et al., 1986; Brazel et al., 1987). As demonstrated in Table A1, there is a higher concentration of glycine in the *S. ehrenbergi* collagen than in non-fibrillar collagen (type IV), further validating that the former is a fibrillar form of collagen.

Table A1 expands on the amino acid differences presented in Table 1. The differences in the amino acid composition between the various types of collagen lends further validates the interpretations made on the structure of the fibrillar collagen described here.

APPENDIX 2

Structural comparison of fibrillar and network-forming collagens

Evident differences can be seen in the X-ray diffraction (XRD) patterns obtained from type IV collagen extracted from the wall of the dogfish egg case when compared with those from fibrillar collagens, such as type I and II and the mesenterial collagen from *S. ehrenbergi*. A detailed XRD analysis on type IV collagen can be found in Gathercole et al. (1993) and Knupp and Squire (1998). Electron microscopy and XRD information from these publications indicates a marked difference between these datasets from type IV and fibrillar (type I and II) collagen. For instance, TEM images from type IV collagen from the dogfish egg case show an alternating banding pattern every 32 nm (Knupp and Squire, 1988). This banding pattern is considerably different from fibrillar collagens, in that there are more discreet striations within the D-periodic repeat (67 nm) in fibrillar collagens.

Similar differences in XRD patterns can be observed. For example, the XRD patterns in type IV collagen show a principle repeat of 81.2 nm (Knupp and Squire, 1998), whereas those from the collagen fibers from *S. ehrenbergi* show a principle repeat of 66 nm. This further validates the use of phase information from mammalian fibrillar collagen (type I and II) to derive one-dimensional electron density maps for the collagen fibers from *S. ehrenbergi*.

Acknowledgements

We thank the staff and scientists of the BioCAT group, and M. Weis for assistance with field and laboratory work. We acknowledge the staff of the Interuniversity Institute for Marine Sciences in Eilat (IUI) for the use of their facilities.

Competing interests

The authors declare no competing or financial interests.

Author contributions

Conceptualization: J.P.R.O.O., I.S., D.B., Y.B.; Methodology: J.P.R.O.O., I.S., R.S.M., Y.K., D.B., Y.B.; Formal analysis: J.P.R.O.O., I.S., R.S.M., Y.K., D.B., Y.B.; Investigation: J.P.R.O.O., I.S., R.S.M., O.A., Y.M., D.B., Y.B.; Resources: J.P.R.O.O., Y.B.; Data curation: J.P.R.O.O.; Writing - original draft: J.P.R.O.O., I.S., O.A., Y.M., Y.B.; Writing - review & editing: J.P.R.O.O., I.S., R.S.M., Y.M., D.B., Y.B.; Visualization: J.P.R.O.O., R.S.M.; Supervision: J.P.R.O.O., Y.B.; Project administration: J.P.R.O.O., Y.B.; Funding acquisition: J.P.R.O.O., D.B., Y.B.

Funding

Use of the Advanced Photon Source was supported by the US Department of Energy, Basic Energy Sciences, Office of Science, under contract no. W-31-109-ENG-38. BioCAT is a National Institutes of Health-supported Research Center RR-08630. This research also used resources of the Advanced Photon Source, a US Department of Energy (DOE) Office of Science User Facility operated for the DOE Office of Science by Argonne National Laboratory under contract no. DE-AC02-06CH11357. Use of BioCARS was supported by the National Institute of General Medical Sciences of the National Institutes of Health under grant number R24GM111072. The content is solely the responsibility of the authors and does not necessarily reflect the official views of the National Institutes of Health. This work was also supported by the National Science Foundation (grant MCB-0644015 CAREER) and this material is based upon work supported by, or in part by, the US Army Research Laboratory and the US Army Research Office under contract/grant number W911NF-11-2-0018-P00002. This research was also supported by the Israeli Ministry of Science (grant 00040047000 to D.B.) and the Israel Cohen Chair in Environmental Zoology (to Y.B.). Deposited in PMC for release after 12 months.

References

Antipova, O. and Orgel, J. P. R. O. (2010). In situ D-periodic molecular structure of type II collagen. *J. Biol. Chem.* **285**, 7087-7096.

Antipova, O. and Orgel, J. P. R. O. (2012). Non-enzymatic decomposition of collagen fibers by a biglycan antibody and a plausible mechanism for rheumatoid arthritis. *PLoS ONE* **7**, e32241.

Barrea, R. A., Antipova, O., Gore, D., Heurich, R., Vukonich, M., Kujala, N. G., Irving, T. C. and Orgel, J. P. R. O. (2014). X-ray micro-diffraction studies on biological samples at the BioCAT Beamline 18-ID at the Advanced Photon Source. *J. Synchrotron Radiat.* **21**, 1200-1205.

Brazel, D., Oberbäumer, I., Dieringer, H., Babel, W., Glanville, R. W., Deutzmann, R. and Kühn, K. (1987). Completion of the amino acid sequence of the α1 chain of human basement membrane collagen (type iv) reveals 21 non-triplet interruptions located within the collagenous domain. *FEBS J.* **168**, 529-536.

Bütikofer, U., Fuchs, D., Bosset, J. O. and Gmür, W. (1991). Automated HPLC-amino acid determination of protein hydrolysates by precolumn derivatization with OPA and FMOC and comparison with classical ion exchange chromatography. *Chromatographia* **31**, 441-447.

Curis, E., Nicolis, I., Moinard, C., Osowska, S., Zerrouk, N., Bénazeth, S. and Cynober, L. (2005). Almost all about citrulline in mammals. *Amino Acids* **29**, 177-205.

Danto, M. I. and Woo, S. L.-Y. (1993). The mechanical properties of skeletally mature rabbit anterior cruciate ligament and patellar tendon over a range of strain rates. *J. Orthop. Res.* **11**, 58-67.

Dykstra, M. J. and Reuss, L. E. (2003). *Biological Electron Microscopy Theory, Techniques, and Troubleshooting*. Boston, MA: Springer US.

Exposito, J.-Y., Larroux, C., Cluzel, C., Valcourt, U., Lethias, C. and Degnan, B. M. (2008). Demosponge and sea anemone fibrillar collagen diversity reveals the early emergence of A/C clades and the maintenance of the modular structure of type V/XI collagens from sponge to human. *J. Biol. Chem.* **283**, 28226-28235.

Exposito, J.-Y., Valcourt, U., Cluzel, C. and Lethias, C. (2010). The fibrillar collagen family. *Int. J. Mol. Sci.* **11**, 407-426.

Fabricius, K. and Alderslade, P. (2001). *Soft Corals and Sea Fans: A Comprehensive Guide to the Tropical Shallow Water Genera of the Central-West Pacific, the Indian Ocean and the Red Sea*. Townsville: Australian Institute of Marine Science.

Fautin, D. G. and Mariscal, R. N. (1991). *Cnidaria: Anthozoa*. New York: Wiley-Liss.

Fung, Y. C. and Liu, S. Q. (1995). Determination of the mechanical properties of the different layers of blood vessels in vivo. *Proc. Natl Acad. Sci. USA* **92**, 2169-2173.

Gathercole, L., Atkins, E., Goldbeck-Wood, E. and Barnard, K. (1993). Molecular bending and networks in a basement membrane-like collagen: packing in dogfish egg capsule collagen. *Int. J. Biol. Macromol.* **15**, 81-88.

Glanville, R. W. (1987). Type IV collagen. In *Structure and Function of Collagen Types* (ed. R. Mayne), pp. 43-79. Orlando, FL: Academic Press. ISBN: 978-0-12-481280-2

Höhne, E. and Rossmann, M. G. (ed.) (1973). The molecular replacement method. A collection of papers on the use of non-crystallographic symmetry. *Cryst. Res. Technol.* **8**, K51.

Knupp, C. and Squire, J. (1998). X-ray diffraction analysis of the 3D organization of collagen fibrils in the wall of the dogfish egg case. *Proc. R. Soc. B* **265**, 2177-2186.

Mandelberg, Y., Benayahu, D. and Benayahu, Y. (2016). Octocoral *Sarcophyton auritum* Verseveldt & Benayahu, 1978: microanatomy and presence of collagen fibers. *Biol. Bull.* **230**, 68-77.

McDowell, L. M., Burzio, L. A., Waite, J. H. and Schaefer, J. (1999). Rotational echo double resonance detection of cross-links formed in mussel byssus under high-flow stress. *J. Biol. Chem.* **274**, 20293-20295.

Nelson, D. L., Cox, M. M., and Lehninger A. L. eds. (2003). *Lehninger Principles of Biochemistry*, 3 edn., Vol. 7. New York, NY: Worth Publ, printing edition. OCLC: 249106180.

Orgel, J. P., Wess, T. J. and Miller, A. (2000). The in situ conformation and axial location of the intermolecular cross-linked non-helical telopeptides of type I collagen. *Structure* **8**, 137-142.

Orgel, J. P. R. O., Irving, T. C., Miller, A. and Wess, T. J. (2006). Microfibrillar structure of type I collagen *in situ*. *Proc. Natl Acad. Sci. USA*, **103**, 9001-9005.

Ortolani, F. and Marchini, M. (1995). Cartilage type II collagen fibrils show distinctive negative-staining band patterns differences between type II and type I unfixed or glutaraldehyde-fixed collagen fibrils. *J. Electron. Microsc.* **44**, 365-375.

Petruska, J. A. and Hodge, A. J. (1964). A subunit model for the tropocollagen macromolecule. *Proc. Natl Acad. Sci. USA* **51**, 871-876.

Provenzano, P. P. and Vanderby, R., Jr. (2006). Collagen fibril morphology and organization: implications for force transmission in ligament and tendon. *Matrix Biol.* **25**, 71-84.

Ross, M. H. and Pawlina, W. (2006). *Histology: A Text and Atlas: With Correlated Cell and Molecular Biology*, 5th edn. Baltimore, MD: Lippincott Wiliams & Wilkins.
Schneider, C. A., Rasband, W. S. and Eliceiri, K. W. (2012). NIH image to ImageJ: 25 years of image analysis. *Nat. Methods* **9**, 671-675.
Schwarz, U., Schuppan, D., Oberbäumer, I., Glanville, R. W., Deutzmann, R., Timpl, R. and Kühn, K. (1986). Structure of mouse type IV collagen. *FEBS J.* **157**, 49-56.
Scott, J. E. (1990). Proteoglycan:collagen interactions and subfibrillar structure in collagen fibrils. Implications in the development and ageing of connective tissues. *J. Anat.* **169**, 23-35.
Sella, I. (2012). *Biological, biochemical, and mechanical properties of collagen fibers of the soft coral Sarcophyton ehrenbergi. PhD thesis*, Tel-Aviv University, Tel-Aviv, Israel.
Sharabi, M., Mandelberg, Y., Benayahu, D., Benayahu, Y., Azem, A. and Haj-Ali, R. (2014). A new class of bio-composite materials of unique collagen fibers. *J. Mech. Behav Biomed. Mater.* **36**, 71-81.
Sharabi, M., Benayahu, D., Benayahu, Y., Isaacs, J. and Haj-Ali, R. (2015). Laminated collagen-fiber bio-composites for soft-tissue bio-mimetics. *Compos. Sci. Technol.* **117**, 268-276.
Sharabi, M., Varssano, D., Eliasy, R., Benayahu, Y., Benayahu, D. and Haj-Ali, R. (2016). Mechanical flexure behavior of bio-inspired collagen-reinforced thin composites. *Compos. Struct.* **153**, 392-400.
Swatschek, D., Schatton, W., Müller, W. and Kreuter, J. (2002). Microparticles derived from marine sponge collagen (SCMPs): preparation, characterization and suitability for dermal delivery of all-trans retinol. *Eur. J. Pharm, Biopharm.* **54**, 125-133.
Tickle, I. J. and Driessen, H. P. C. (1996). Molecular replacement using known structural information. In *Crystallographic Methods and Protocols* (ed. C. Jones, B. Mulloy and M. R. Sanderson), pp. 173-203. Totowa, NJ: Humana Press.
Vogel, S. (2013). *Comparative Biomechanics: Life's Physical World*, 2nd edn. Princeton, NJ: Princeton University Press.
Wess, T. J. and Orgel, J. P. (2000). Changes in collagen structure: drying, dehydrothermal treatment and relation to long term deterioration. *Thermochimica Acta* **365**, 119-128.
White, J. F., Werkmeister, J. A., Darby, I. A., Bisucci, T., Birk, D. E. and Ramshaw, J. A. M. (2002). Collagen fibril formation in a wound healing model. *J. Struct. Biol.* **137**, 23-30.